

Pressure-driven high-to-low spin transition in the bimetallic quantum magnet [Ru₂(O₂CMe)₄]₃[Cr(CN)₆]

K. R. O'Neal,¹ Z. Liu,² Joel S. Miller,³ R. S. Fishman,⁴ and J. L. Musfeldt¹¹*Department of Chemistry, University of Tennessee, Knoxville, Tennessee 37996, USA*²*Geophysical Laboratory, Carnegie Institution of Washington, Washington, D.C. 20015, USA*³*Department of Chemistry, University of Utah, Salt Lake City, Utah 84112, USA*⁴*Materials Science and Technology Division, Oak Ridge National Laboratory, Oak Ridge, Tennessee 37831, USA*

(Received 27 June 2014; revised manuscript received 12 August 2014; published 2 September 2014)

Synchrotron-based infrared and Raman spectroscopies were brought together with diamond anvil cell techniques and an analysis of the magnetic properties to investigate the pressure-induced high \rightarrow low spin transition in [Ru₂(O₂CMe)₄]₃[Cr(CN)₆]. The extended nature of the diruthenium wave function combined with coupling to chromium-related local lattice distortions changes the relative energies of the π^* and δ^* orbitals and drives the high \rightarrow low spin transition on the mixed-valence diruthenium complex. This is a rare example of an externally controlled metamagnetic transition in which both spin-orbit and spin-lattice interactions contribute to the mechanism.

DOI: [10.1103/PhysRevB.90.104301](https://doi.org/10.1103/PhysRevB.90.104301)

PACS number(s): 78.30.-j, 75.50.Xx, 75.30.Kz, 78.20.H-

I. INTRODUCTION

Magnetic crossover transitions modulated by external stimuli such as temperature, magnetic field, pressure, and light are the subject of contemporary interest [1]. These transitions can be as simple as low \leftrightarrow high spin in an isolated molecule or as complex as antiferromagnetic \leftrightarrow ferromagnetic, metamagnetic, and quantum critical processes in extended solids [2–12]. Spin crossovers in 4- and 5d-containing compounds are particularly interesting because spin-orbit coupling competes with electron correlations to reveal exotic properties [13–19].

The mixed-metal quantum antiferromagnet [Ru₂(O₂CMe)₄]₃[Cr(CN)₆] (Me = CH₃) attracted our attention due to its sensitivity to various external stimuli combined with the unusual interpenetrating lattice structure [20–29]. As summarized in the schematic phase diagram of Fig. 1, temperature drives a magnetic ordering transition at 33 K, below which the magnetic alignment of each sublattice possesses three diruthenium spins with easy axes along face diagonals opposed by the Cr spin along the body diagonal [20–27]. There is practically no coupling between the two sublattices so there are many degenerate configurations, which can be aligned by an 0.08 T magnetic field [24]. This compound thus represents an interesting example of a three-dimensional system (Fig. 2) with frustration that can be lifted by external stimuli. Pressure triggers a different kind of magnetic crossover, with 0.8 GPa driving the high \rightarrow low spin antiferromagnetic transition [22,25]. Previous authors [22,25] argue that the collapse of the high spin state is an effective Ru₂^{II/III} high ($S = 3/2$) \rightarrow low spin ($S = 1/2$) transition. However, more complicated mechanisms involving magnetoelastic coupling, electron transfer, and charge ordering have not been rigorously tested. The role of spin-orbit coupling is also relatively unexplored.

In order to distinguish between these magnetic crossover mechanisms, we ventured beyond high magnetic field spectroscopy [29] to investigate the infrared and Raman response of [Ru₂(O₂CMe)₄]₃[Cr(CN)₆] under pressure. Combining our

findings with displacement patterns and anticipated mode trends for (i) an isolated on-site high \rightarrow low spin transition, (ii) a spin-lattice assisted crossover, and (iii) electron transfer (or charge ordering) induced spin transition reveals that while the spin transition takes place on the Ru dimer, it is enabled by cooperative local lattice distortions around the Cr center. Due to its mixed II/III valence, the $S = 3/2$ state of the diruthenium complex lies at the borderline of stability compared to the $S = 1/2$ configuration. We propose a mechanism in which the cooperative lattice distortion around the Cr ion destabilizes the $S = 3/2$ state by changing the effective field at the diruthenium complex, a process that inverts the π^* and δ^* orbitals and leads to the $S = 1/2$

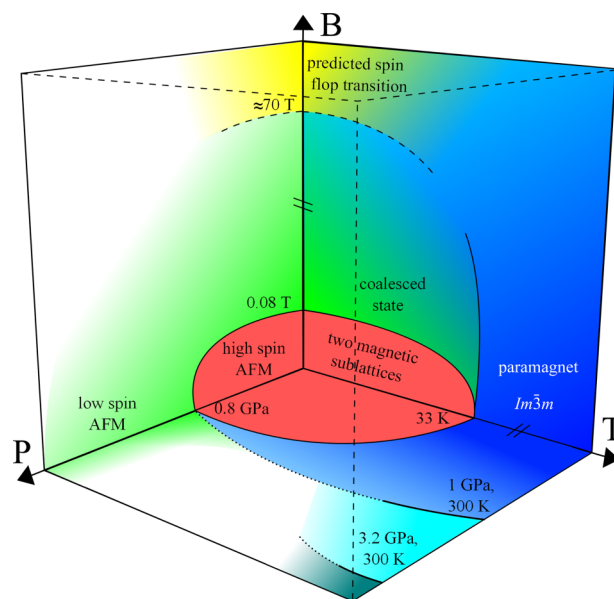


FIG. 1. (Color online) Schematic temperature-pressure-magnetic field phase diagram for [Ru₂(O₂CMe)₄]₃[Cr(CN)₆]. Different magnetic states are revealed in response to various external stimuli [20–29]. The regimes obtained from an analysis of local lattice distortions (this work) are also represented.

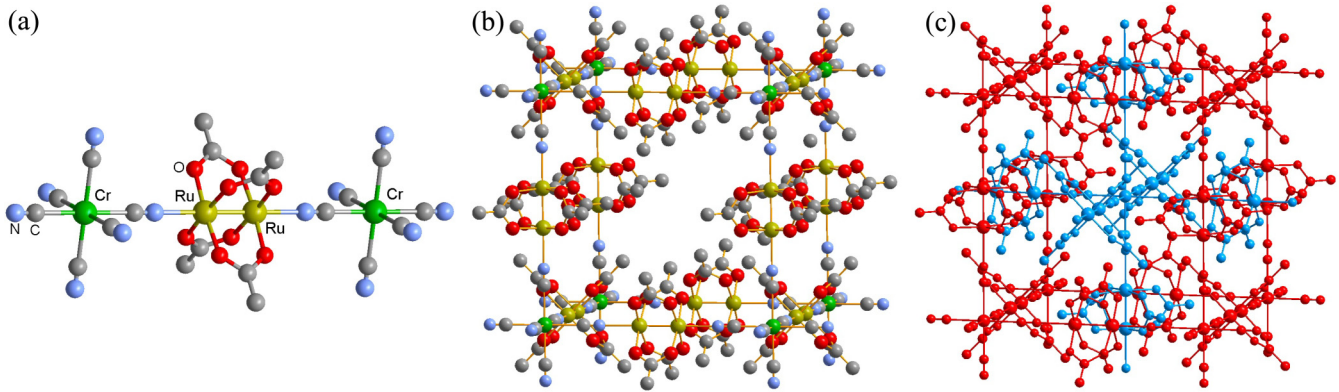


FIG. 2. (Color online) (a) View of the $\text{Cr}^{\text{III}}\text{-Ru}^{\text{II/III}}\text{-Cr}^{\text{III}}$ structural linkage. Each Cr^{III} center of $[\text{Cr}(\text{CN})_6]^{3-}$ and each mixed-valent $\text{Ru}_2^{\text{II/III}}$ unit in the $[\text{Ru}_2(\text{O}_2\text{CMe})_4]^+$ paddle-wheel complex has a spin $S = 3/2$ [20]. The 3 and 4d metal centers bring in electron-electron and spin-orbit interactions, respectively. Superexchange between the mixed-metal centers relies on diamagnetic cyan ligands. (b) The single, noninterpenetrating sublattice and (c) a diagram of the two interpenetrating cubic lattices (red and blue) in body-centered cubic $[\text{Ru}_2(\text{O}_2\text{CMe})_4]_3[\text{Cr}(\text{CN})_6]$ [20,30]. Hydrogen atoms are omitted for clarity. The lattice constant, a , is 13.3 Å [20]. $[\text{Ru}_2(\text{O}_2\text{CMe})_4]_3[\text{Cr}(\text{CN})_6]$ is the only known system with two weakly interacting ferrimagnetic lattices occupying the same volume that are almost completely decoupled [24].

state. Crossover mechanisms involving both spin-orbit and spin-lattice interactions may also be important in other 4- and 5d-containing magnets. Piezomagnetism and pressure-tunable spin-orbit coupling may emerge in these systems as well.

II. METHODS

Polycrystalline $[\text{Ru}_2(\text{O}_2\text{CMe})_4]_3[\text{Cr}(\text{CN})_6]$ was prepared as described previously [20]. The sample was loaded into a pressure medium like vacuum grease in order to apply quasi-hydrostatic pressure. Ruby fluorescence was used to measure pressure [31]. Raman measurements (0.5 cm^{-1} resolution) were performed with a custom micro-Raman system including a spectrograph, a CCD detector, and a 532 nm diode pumped solid state laser, with power below 1 mW to prevent sample degradation. Due to the small sample size and $300\text{ }\mu\text{m}$ diamond culets, the National Synchrotron Light Source at Brookhaven National Laboratory was used for its high brightness infrared light [32]. Infrared measurements were taken with a resolution of 1 cm^{-1} . In prior work, the vibrational properties at ambient pressure were found not to change at the 33 K magnetic ordering transition; there are also no signatures of the 0.08 T magnetic coalescence transition [29]. This connects the 300 K high pressure spectral measurements to the low temperature magnetic crossover.

To model the field- and pressure-induced phase transitions in this material, we assume as a starting point that the moments of each sublattice are rigid with no internal degrees of freedom. Each sublattice moment is confined to a cubic diagonal (with eight possible orientations) by the strong easy-plane anisotropy of the diruthenium paddle wheel. Hence the partition function for the material involves the sum over 8×8 spin configurations. To describe the weak nonrigid distortion of each sublattice, a field-dependent susceptibility is added to each sublattice spin. Although their orbital overlap is negligible, the two ferrimagnetic sublattices are antiferromagnetically coupled by dipolar interactions [24]. This model successfully describes the coalescence transition

at low temperatures with a 0.08 T field and indicates that the sublattice spin drops by about half above a pressure of 0.8 GPa.

III. RESULTS AND DISCUSSION

Figure 3 displays our spectroscopic findings. We assign the vibrational features of $[\text{Ru}_2(\text{O}_2\text{CMe})_4]_3[\text{Cr}(\text{CN})_6]$ based upon a symmetry analysis, measurements of model compounds, and comparison with literature data [29,33–37]. The infrared bands near 120 , 360 , and 450 cm^{-1} are associated with the C-Cr-C bend, Cr-C stretch, and Cr-C-N bend of the $[\text{Cr}(\text{CN})_6]^{3-}$ ion, respectively [38]. The $[\text{Ru}_2(\text{O}_2\text{CMe})_4]^+$ paddle-wheel complex also displays a set of well-known vibrational features. For instance, the strong Raman-active peaks at 320 , 360 , and 2150 cm^{-1} are assigned as Ru-Ru, Ru-O, and $\text{C}\equiv\text{N}$ stretching modes, respectively. The strong infrared-active peaks at $\simeq 345$ and 400 cm^{-1} are associated with the Ru-O stretch [29,36,39,40]. The ligands of $[\text{Ru}_2(\text{O}_2\text{CMe})_4]^+$ also display their usual fingerprints; the carboxylate rocking modes between 605 and 625 cm^{-1} are important in the following discussion. Compression modifies all of these features. Some modes display slope changes, frequency shifts, and changes in splitting pattern, whereas others harden systematically [Figs. 3(e)–3(h)] [41]. Taken together, the frequency vs pressure trends uncover local lattice distortions near 1 and 3.2 GPa. The former coincides with the high \rightarrow low spin transition in $[\text{Ru}_2(\text{O}_2\text{CMe})_4]_3[\text{Cr}(\text{CN})_6]$, which appears at 0.8 GPa at low temperature. The latter has not been previously observed. It is not known whether the 3.2 GPa structural distortion (discussed below) has a magnetic component.

We extract information about the pressure-driven local lattice distortions by bringing the vibrational response together with mode assignment and displacement pattern information (Fig. 3). Strikingly, compression through the 1 GPa transition affects only modes related to $[\text{Cr}(\text{CN})_6]^{3-}$, as evidenced by the sensitivity of the 120 , 360 , 450 , and 2150 cm^{-1} peaks. Trends

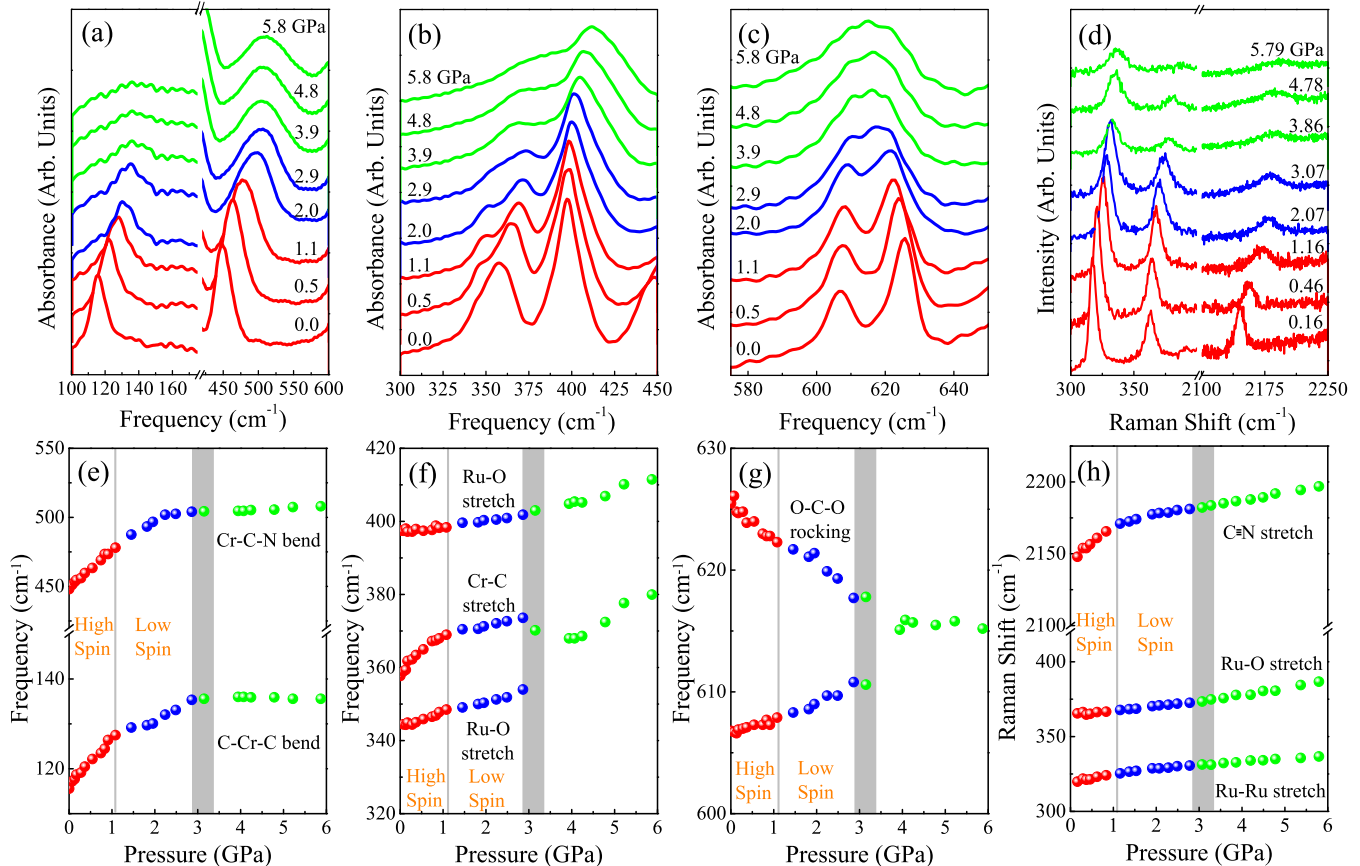


FIG. 3. (Color online) Closeup views of the infrared (a,b,c) and Raman (d) response of $[\text{Ru}_2(\text{O}_2\text{CMe})_4]_3[\text{Cr}(\text{CN})_6]$ as a function of pressure at 300 K. (e,f,g,h) Frequency vs pressure trends showing how the various modes change through the pressure-driven transitions (denoted by the gray vertical lines at 1 and 3.2 GPa). The mode assignments are indicated.

in the $\text{C}\equiv\text{N}$ stretch anticorrelate with distance, so overall hardening implies a longer bond. By contrast, the modes associated with the $[\text{Ru}_2(\text{O}_2\text{CMe})_4]^+$ paddle-wheel complex are unperturbed. This pattern of flexible $[\text{Cr}(\text{CN})_6]^{3-}$ building blocks and rigid $[\text{Ru}_2(\text{O}_2\text{CMe})_4]^+$ paddle-wheel complexes is familiar. Other external stimuli produce the same outcome: soft $[\text{Cr}(\text{CN})_6]^{3-}$ octahedra and stiff $[\text{Ru}_2(\text{O}_2\text{CMe})_4]^+$ units [29]. Pressure is different than temperature or magnetic field in that it acts directly on bond lengths and angles to modify exchange interactions [42,43]. The high \rightarrow low spin transition at 1 GPa is different than the field-induced coalescence transition at 0.08 T in that the most significant spin-lattice coupling takes place under pressure [44].

The 3.2 GPa transition is broader and more sluggish than that near 1 GPa. Furthermore, it involves the equatorial carboxylate ligands in the diruthenium complex rather than the Ru-Ru-based mode. The well-known displacements of the $[\text{Cr}(\text{CN})_6]^{3-}$ cluster do not participate. It's unfortunately hard to say much about the mechanism (other than that it involves local lattice distortions on the periphery of the Ru dimer) without the benefit of magnetic property measurements. Several other molecule-based magnets display pressure-induced local lattice distortions in this range [45,46], making the exploration of higher pressure magnetic properties of general interest.

Analysis of these frequency-pressure trends reveals that the 0.8 GPa high \rightarrow low spin transition in $[\text{Ru}_2(\text{O}_2\text{CMe})_4]_3[\text{Cr}(\text{CN})_6]$ is more complicated than previously supposed. It is particularly surprising that the Ru-containing modes (especially the Raman-active Ru-Ru-based stretching mode at 320 cm⁻¹ [Fig. 3(h)]) are completely insensitive to the crossover. This behavior rules out charge ordering mechanisms on the $[\text{Ru}_2(\text{O}_2\text{CMe})_4]^+$ paddle-wheel complex through the transition. Moreover, the absence of large frequency differences in the Cr-related modes eliminates processes involving inhomogeneous charge disproportionation involving $[\text{Cr}(\text{CN})_6]^{3-}$ [47]. An isolated high \rightarrow low spin mechanism (within a rigid electronic structure) can also be ruled out because the lattice clearly participates in the 1 GPa transition [48].

As discussed below, the local lattice distortions facilitate the magnetic crossover in $[\text{Ru}_2(\text{O}_2\text{CMe})_4]_3[\text{Cr}(\text{CN})_6]$. In fact, they occur first [49]. But why does magnetoelastic coupling involve modes related to $[\text{Cr}(\text{CN})_6]^{3-}$? If the 1 GPa magnetic crossover occurs on the Ru dimer, why should these modes change at all? Could it be that the high \rightarrow low spin transition involves the Cr centers instead?

There are two reasons to rule out this possibility. First, the net spin of each sublattice below the coalescence transition opposes the Cr spins. For classical spins and infinite easy-plane

anisotropy on the diruthenium paddle wheel, the net spin of each sublattice is $S_{\text{tot}} = (\sqrt{6} - 1)S \approx 2.18$ per formula unit [24]. Due to the finite anisotropy of the paddle wheel, this is 18% larger than the value $S_{\text{tot}} = 1.85$ extracted from the field dependence of the magnetization using the model described above. A $S = 3/2 \rightarrow 1/2$ transition on the Cr spin would increase the sublattice spin by about 50%, in disagreement with the observed decrease of S_{tot} above 0.8 GPa. Second, an octahedral Cr(III) center has never been observed in the low spin $S = 1/2$ state.

On the other hand, the mixed-valence $\text{Ru}_2(\text{II/III})$ complex can undergo a high \rightarrow low spin transition or exhibit intermediate admixed spin behavior [50–55]. This is because the presence of spin-orbit coupling causes the π^* and δ^* orbital energies to be quite close [50–55], a situation that amplifies the effect of small perturbations. Consequently, spin-admixed ruthenium compounds occur [52]. Here, we recall that the valence configuration for the 11 electrons in the $S = 3/2$ state of the Ru dimer is generally accepted to be $\sigma^2\pi^4\delta^2\pi^*\delta^*1$ [50]. We will abbreviate this configuration using the last two antibonding orbitals with the relevant energy order and occupation. For the most likely high spin arrangement, this is “ $\pi^*\delta^*1$.” The order and occupancy of the π^* and δ^* orbitals also determines the nature of the low spin state.

Our situation is similar to that described above. Due to the extended nature of the $4d$ orbitals, the state of the $[\text{Ru}_2(\text{O}_2\text{CMe})_4]^+$ complex is very sensitive to changes in ligand fields. In particular, variations in the axial $\cdots\text{N}\cdots$ ligand are known to alter the spin states of compounds containing the $[\text{Ru}_2(\text{O}_2\text{CMe})_4]^+$ paddle wheel [54,56–58]. It follows that the balance between the energies of the orbital states can be easily shifted by small changes in the ligand fields. The cooperative local lattice distortions around the Cr site provide just such a destabilizing change. According to Ref. [22], compression reduces the $\text{Ru}\cdots\text{N}$ distance by 5.5%, enhancing the π^* orbital interaction and increasing their energy (Fig. 4) relative to the δ^* orbital. This process inverts the π^* and δ^* levels and leads to a $\delta^*\pi^*$ low spin state.

While the high spin $\pi^*\delta^*$ to low spin $\delta^*\pi^*$ scenario is most reasonable, there are alternate valence configuration patterns that can produce a spin crossover. The schematic diagram in Fig. 4 accounts for these as well. For instance, the high spin ground state could be $\delta^*\pi^*$, and under pressure, the energy of the π^* orbital might increase such that the low spin configuration becomes $\delta^*\pi^*$ simply due to an increasingly substantial energy difference between states. That said, $\pi^*\delta^*$ is generally accepted as the high spin ground state [50], so the competition between it and low spin $\delta^*\pi^*$ is most likely. Finally, we point out that some papers have suggested that the low spin state of Ru-based complexes can be $\pi^*\pi^*$ rather than $\delta^*\pi^*$. This narrative implies that the π^* orbital lies lower than the δ^* orbital [51,59].

With spin on the diruthenium complex decreasing from $S = 3/2$ to $S = 1/2$ at 0.8 GPa, the sublattice spin changes sign and points along the Cr spin direction. The total sublattice spin S_{tot} depends on the anisotropic exchange between the low-spin complex and the Cr ion. If the exchange interactions between the three inequivalent $S = 1/2$ diruthenium complexes and the $S = 3/2$ Cr ion are (J_2, J_1, J_1) , (J_1, J_2, J_1) , and (J_1, J_1, J_2) for spins separated by $(a/2)\mathbf{x}$, $(a/2)\mathbf{y}$, and $(a/2)\mathbf{z}$,

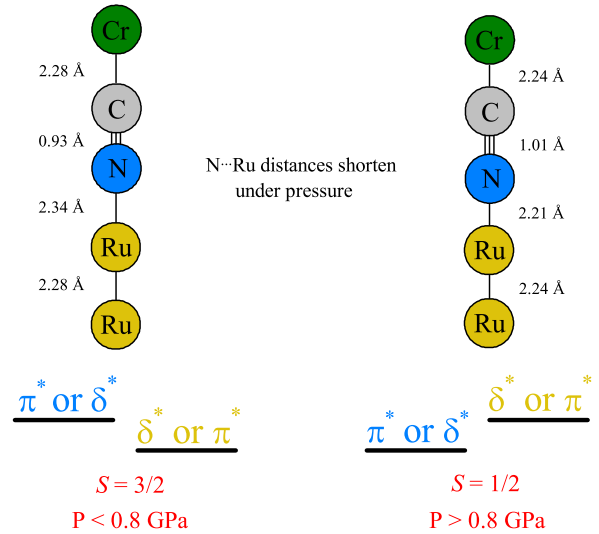


FIG. 4. (Color online) Schematic of bond lengths along the superexchange pathway at ambient pressure conditions and under compression [22] along with the relative orbital energies on the $[\text{Ru}_2(\text{O}_2\text{CMe})_4]^+$ complex. The orbital configuration of the high spin phase is probably $\pi^*\delta^*$ [50], although $\delta^*\pi^*$ is also possible. The orbital state of the low spin phase is either $\delta^*\pi^*$ or $\pi^*\pi^*$. As discussed in the text, a high spin $\pi^*\delta^*$ to low spin $\delta^*\pi^*$ crossover is most probable. This orbital inversion under compression is made possible by cooperative local lattice distortions on the $[\text{Cr}(\text{CN})_6]^{3-}$ sites.

respectively, then the total spin of the sublattice per Cr site along a diagonal will be

$$S_{\text{tot}} = \frac{3}{2} - \frac{\sqrt{3}}{2}(\sqrt{2}\cos\theta + \sin\theta). \quad (1)$$

Here, $\tan\theta = \sqrt{2}J_2/J_1$, and a is the lattice constant (13.3 Å). So $S_{\text{tot}} \rightarrow 0.28$ for $J_2 \rightarrow 0$ and $S_{\text{tot}} \rightarrow 0.63$ for $J_1 \rightarrow 0$. This is an experimental observation of a pressure-induced high \rightarrow low spin transition for a diruthenium complex, although there are many instances of compression-induced spin crossovers in solid state systems [60–64]. Anisotropic exchange interactions are important in other heavy-atom organic magnets as well [65].

Of course, spin-orbit coupling on the $[\text{Ru}_2(\text{O}_2\text{CMe})_4]^+$ complex plays an essential role in this high \rightarrow low spin transition by creating the balance between the nearly degenerate π^* and δ^* levels. Our work therefore uncovers one of the few examples [66] in which spin-orbit coupling can be reversibly tuned and potentially controlled by a pressure-driven change in ligand fields. Similar interactions may drive magnetic crossovers in other 4- and 5d-containing materials. In fact, compounds with 5d centers may be even more sensitive to pressure than 4d systems due to the more extended orbitals.

IV. SUMMARY

To summarize, an analysis of the high pressure magnetic and vibrational properties of the bimetallic quantum magnet $[\text{Ru}_2(\text{O}_2\text{CMe})_4]_3[\text{Cr}(\text{CN})_6]$ reveals how a pressure-induced high \rightarrow low spin crossover at the diruthenium site is driven by the extended nature of the $4d$ orbitals on the diruthenium complex combined with spin-lattice interactions emanating

from $[\text{Cr}(\text{CN})_6]^{3-}$. Looking at it another way, pressure (and probably strain) reversibly control local lattice distortions in the Cr · · · C · · · N · · · Ru exchange pathway, determining the ligand field around the Ru sites, the balance between the π^* and δ^* orbitals, and whether the high or low spin state is exposed. This is interesting because $[\text{Ru}_2(\text{O}_2\text{CMe})_4]_3[\text{Cr}(\text{CN})_6]$ is an example of a potentially much broader class of 4- and 5d-containing materials in which both spin-orbit and spin-lattice interactions contribute to the crossover mechanism. Whether pressure (or strain) can modulate the spin state in thin film form [67] is an open question, but these effects can form the basis for new types of piezo- and electromagnets [68].

ACKNOWLEDGMENTS

This research was funded by the National Science Foundation under Grants No. DMR-1063880 (J.L.M.) and No. DMR-11063630 (J.S.M.) as well as by the US Department of Energy, Office of Basic Energy Sciences, Materials Sciences and Engineering Division (R.S.F.). Work at the National Synchrotron Light Source at Brookhaven National Laboratory was supported by the US Department of Energy under Contract No. DE-AC98-06CH10886. The use of U2A beamline was supported by COMPRES under NSF Cooperative Agreement EAR 11-57758 and CDAC (DE-FC03-03N00144).

-
- [1] *Spin-crossover Materials: Properties and Applications*, edited by M. A. Halcrow (Wiley and Sons, New York, 2013).
- [2] M. Verdaguer, A. Bleuzen, V. Marvaud, J. Vaissermann, M. Seuleiman, C. Desplanches, A. Scullier, C. Train, R. Garde, G. Gelly, C. Lomenech, I. Rosenman, P. Veillet, C. Cartier, and F. Villain, *Coord. Chem. Rev.* **190-192**, 1023 (1999).
- [3] M. Verdaguer and G. S. Girolami, in *Magnetism: Molecules to Materials V*, edited by J. S. Miller and M. Drillon (Wiley-VCH, Weinheim, 2005), p. 283.
- [4] E. Coronado, J. R. Galán-Mascarós, C. J. Gómez-Carcía, and V. Laukhin, *Nature (London)* **408**, 447 (2000).
- [5] A. Marvilliers, S. Parsons, E. Rivière, J.-P. Audière, M. Kurmoo, and T. Mallah, *Eur. J. Inorg. Chem.* **2001**, 1287 (2001).
- [6] M. Zentková, Z. Arnold, J. Kamarád, V. Kavečanský, M. Lukáčova, S. Mat'áš, M. Mihalik, M. Mitróová, and A. Zentko, *J. Phys.: Condens. Matter* **19**, 266217 (2007).
- [7] P. A. Goddard, J. Singleton, P. Sengupta, R. D. McDonald, T. Lancaster, S. J. Blundell, F. L. Pratt, S. Cox, N. Harrison, J. L. Manson, H. I. Southerland, and J. A. Schlüter, *New J. Phys.* **10**, 083025 (2008).
- [8] M. Ohba, W. Kaneko, S. Kitagawa, T. Maeda, and M. Mito, *J. Am. Chem. Soc.* **130**, 4475 (2008).
- [9] Y. Narumi, N. Terada, Y. Tanaka, M. Iwaki, K. Katsumata, K. Kindo, H. Kageyama, Y. Ueda, H. Toyokawa, T. Ishikawa, and H. Kitamura, *J. Phys. Soc. Jpn.* **78**, 043702 (2009).
- [10] T. V. Brinzari, P. Chen, Q.-C. Sun, J. Liu, L.-C. Tung, Y. J. Wang, J. A. Schlüter, J. Singleton, J. L. Manson, M.-H. Whangbo, A. P. Litvinchuk, and J. L. Musfeldt, *Phys. Rev. Lett.* **110**, 237202 (2013).
- [11] Ö. Günaydin-Şen, P. Chen, J. Fosso-Tande, T. L. Allen, J. Cherian, T. Tokumoto, P. M. Lahti, S. McGill, R. J. Harrison, and J. L. Musfeldt, *J. Chem. Phys.* **138**, 204716 (2013).
- [12] P. Chen, B. S. Holinsworth, K. R. O'Neal, T. V. Brinzari, D. Mazumdar, Y. Q. Wang, S. McGill, R. J. Cava, B. Lorenz, and J. L. Musfeldt, *Phys. Rev. B* **89**, 165120 (2014).
- [13] W. Kosaka, K. Nomura, K. Hashimoto, and S. Ohkoshi, *J. Am. Chem. Soc.* **127**, 8590 (2005).
- [14] S. A. Baudron, P. Batail, C. Coulon, R. Clerac, E. Canadell, V. Laukhin, R. Melzi, P. Wzietek, D. Jerome, P. Auban-Senzier, and S. Ravy, *J. Am. Chem. Soc.* **127**, 11785 (2005).
- [15] D. R. Allan, A. J. Blake, D. Huang, T. J. Prior, and M. Schröder, *Chem. Commun.* **2006**, 4081 (2006).
- [16] M. G. Hilfiger, M. Chen, T. V. Brinzari, T. M. Nocera, M. Shatruk, D. T. Petais, J. L. Musfeldt, C. Achim, and K. R. Dunbar, *Angew. Chem. Int. Ed.* **49**, 1410 (2010).
- [17] X.-Y. Wang, C. Avendaño, and K. R. Dunbar, *Chem. Soc. Rev.* **40**, 3213 (2011).
- [18] X. Feng, J. Liu, T. D. Harris, S. Hill, and J. R. Long, *J. Am. Chem. Soc.* **134**, 7521 (2012).
- [19] K. Tarafder, S. Kanungo, P. M. Oppeneer, and T. Saha-Dasgupta, *Phys. Rev. Lett.* **109**, 077203 (2012).
- [20] T. E. Vos, Y. Liao, W. W. Shum, J.-H. Her, P. W. Stephens, W. M. Reiff, and J. S. Miller, *J. Am. Chem. Soc.* **126**, 11630 (2004).
- [21] J. S. Miller, T. E. Vos, and W. W. Shum, *Adv. Mater.* **17**, 2251 (2005).
- [22] W. W. Shum, J.-H. Her, P. W. Stephens, Y. Lee, and J. S. Miller, *Adv. Mater.* **19**, 2910 (2007).
- [23] W. W. Shum, J. N. Schaller, and J. S. Miller, *J. Phys. Chem. C* **112**, 7936 (2008).
- [24] R. S. Fishman, S. Okamoto, W. W. Shum, and J. S. Miller, *Phys. Rev. B* **80**, 064401 (2009).
- [25] R. S. Fishman, W. W. Shum, and J. S. Miller, *Phys. Rev. B* **81**, 172407 (2010).
- [26] R. S. Fishman and J. S. Miller, *Phys. Rev. B* **83**, 094433 (2011).
- [27] T. Lancaster, F. L. Pratt, S. J. Blundell, A. J. Steele, P. J. Baker, J. D. Wright, I. Watanabe, R. S. Fishman, and J. S. Miller, *Phys. Rev. B* **84**, 092405 (2011).
- [28] R. S. Fishman, J. Campo, T. E. Vos, and J. S. Miller, *J. Phys.: Condens. Matter* **24**, 496001 (2012).
- [29] T. V. Brinzari, P. Chen, L.-C. Tung, Y. Kim, D. Smirnov, J. Singleton, J. S. Miller, and J. L. Musfeldt, *Phys. Rev. B* **86**, 214411 (2012).
- [30] Y. Liao, W. W. Shum, and J. S. Miller, *J. Am. Chem. Soc.* **124**, 9336 (2002).
- [31] H. K. Mao, P. M. Bell, J. W. Shaner, and D. J. Steinberg, *J. Appl. Phys.* **49**, 3276 (1978).
- [32] G. L. Carr, M. C. Martin, W. R. McKinney, K. Jordan, G. R. Neil, and G. P. Williams, *Nature (London)* **420**, 153 (2002).
- [33] L. H. Jones, *Inorg. Chem.* **2**, 777 (1963); L. H. Jones, M. N. Memering, and B. I. Swanson, *J. Chem. Phys.* **54**, 4666 (1971).
- [34] I. Nakagawa and T. Shimanouchi, *Spectrochim. Acta A* **26**, 131 (1970); I. Nakagawa, *Bull. Chem. Soc. Jpn.* **46**, 3690 (1973).
- [35] O. Zakhariyeva-Pencheva and V. A. Demetiev, *J. Mol. Struct.* **90**, 241 (1982).
- [36] V. M. Miskowski, T. M. Loehr, and H. B. Gray, *Inorg. Chem.* **26**, 1098 (1987).
- [37] S.-K. Park, C.-K. Lee, S.-H. Lee, and N.-S. Lee, *Bull. Korean Chem. Soc.* **23**, 253 (2002).
- [38] The Cr-C stretch and Cr-C-N bend are mixed.

- [39] The second component of Ru-O stretching is expected near 340 cm^{-1} . This is very near (and close to overlapping with) the Cr-C band. We suspect that the Ru-O mode corresponds to the weak feature near 345 cm^{-1} [29,36]. This peak displays a very weak temperature dependence ($<1\text{ cm}^{-1}$), and no field dependence within our error bars, a behavior that is quite similar to the 400 cm^{-1} feature, thus providing an additional support to its assignment [29].
- [40] The location of the $\nu(\text{Ru-N})$ stretch is uncertain. The feature near 280 cm^{-1} likely corresponds to one of the expected weak Ru-O deformation bands, while peaks near 620 and higher energy 690 cm^{-1} are assigned to $\rho(\text{COO})$ rocking and $\delta(\text{COO})$ bend, respectively. The very weak excitation near 945 cm^{-1} corresponds to $\nu(\text{C-C})$ stretch [36]. None of these bands are sensitive to magnetic field [29].
- [41] Here and elsewhere in the text, “hardening” or “blueshifting” refers to a shift to higher energy, whereas “softening” or “redshifting” indicates a shift to lower energy.
- [42] P. W. Anderson, *Solid State Phys.* **14**, 99 (1963).
- [43] J. B. Goodenough, *Magnetism and the Chemical Bond* (Interscience Publishers, New York-London, 1963).
- [44] By contrast, magnetoinfrared and magneto-Raman spectra show no change through the 0.08 T coalescence transition [29].
- [45] J. L. Musfeldt, T. V. Brinzari, J. A. Schlueter, J. L. Manson, A. P. Litvinchuk, and Z. Liu, *Inorg. Chem.* **52**, 14148 (2013).
- [46] K. R. O'Neal, T. V. Brinzari, J. B. Wright, C. Ma, S. Giri, J. A. Schlueter, Q. Wang, P. Jena, Z. Liu, and J. L. Musfeldt, *Sci. Rep.* **4**, 6045 (2014).
- [47] F. D. Hardcastle and I. E. Wachs, *J. Raman Spectrosc.* **21**, 683 (1990).
- [48] These local lattice distortions will strengthen at low temperature.
- [49] This is evidenced by the fact that the lattice distortions set in at higher temperature.
- [50] V. M. Miskowski, M. D. Hopkins, J. R. Winkler, and H. B. Gray, in *Inorganic Electronic Structure and Spectroscopy*, edited by E. I. Solomon and A. B. P. Lever (John Wiley & Sons, Inc., New York, 1999), Vol. 2, p. 343.
- [51] P. Angaridis, A. Cotton, A. Murillo, D. Villagrán, and X. Wang, *J. Am. Chem. Soc.* **127**, 5008 (2005).
- [52] M. C. Barral, S. Herrero, R. Jiménez-Aparicio, M. R. Torres, and F. A. Urbanos, *Angew. Chem. Int. Ed.* **44**, 305 (2005).
- [53] M. C. Barral, T. Gallo, S. Herrero, R. Jiménez-Aparicio, M. R. Torres, and F. A. Urbanos, *Inorg. Chem.* **45**, 3639 (2006).
- [54] M. C. Barral, D. Casanova, S. Herrero, R. Jiménez-Aparicio, M. R. Torres, and F. A. Urbanos, *Chem. Eur. J.* **16**, 6203 (2010).
- [55] M. C. Barral, T. Gallo, S. Herrero, R. Jiménez-Aparicio, M. R. Torres, and F. A. Urbanos, *Chem. Eur. J.* **13**, 10088 (2007).
- [56] J. L. Bear, B. Han, S. Huang, and K. M. Kadish, *Inorg. Chem.* **35**, 3012 (1996).
- [57] F. A. Cotton and A. Yokuchi, *Inorg. Chem.* **37**, 2723 (1998).
- [58] W.-Z. Chen and T. Ren, *Inorg. Chem.* **42**, 8847 (2003).
- [59] M. C. Barral, R. González-Prieto, S. Herrero, R. Jiménez-Aparicio, J. L. Priego, E. C. Royer, M. R. Torres, and F. A. Urbanos, *Polyhedron* **23**, 2637 (2004).
- [60] M. Takano, S. Nasu, T. Abe, K. Yamamoto, S. Endo, Y. Takeda, and J. B. Goodenough, *Phys. Rev. Lett.* **67**, 3267 (1991).
- [61] J.-P. Rueff, C.-C. Kao, V. V. Struzhkin, J. Badro, J. Shu, R. J. Hemley, and H. K. Mao, *Phys. Rev. Lett.* **82**, 3284 (1999).
- [62] F. Aguado, F. Rodríguez, and P. Núñez, *Phys. Rev. B* **76**, 094417 (2007).
- [63] D. P. Kozlenko, N. O. Golosova, Z. Jiráček, L. S. Dubrovinsky, B. N. Savenko, M. G. Tucker, Y. Le Godec, and V. P. Glazkov, *Phys. Rev. B* **75**, 064422 (2007).
- [64] N. O. Golosova, D. P. Kozlenko, L. S. Dubrovinsky, O. A. Drozhzhin, S. Ya. Istomin, and B. N. Savenko, *Phys. Rev. B* **79**, 104431 (2009).
- [65] S. M. Winter, R. T. Oakley, A. E. Kovalev, and S. Hill, *Phys. Rev. B* **85**, 094430 (2012).
- [66] A. Mang, K. Reimann, and S. Rübenacke, *Solid State Commun.* **94**, 251 (1995).
- [67] D. R. Talham and M. W. Meisel, *Chem. Soc. Rev.* **40**, 3356 (2011).
- [68] A. Palić, J. M. Clemente-Juan, B. Tsukerblat, and E. Coronado, *Chem. Sci.* **5**, 3598 (2014).